Science of the Total Environment 772 (2021) 144897

Contents lists available at ScienceDirect

Science of the Total Environment

journal homepage: www.elsevier.com/locate/scitotenv

Rapid sulfate formation from synergetic oxidation of SO_2 by O_3 and NO_2 under ammonia-rich conditions: Implications for the explosive growth of atmospheric $PM_{2.5}$ during haze events in China

Si Zhang [a,b], Dapeng Li [a,b], Shuangshuang Ge [a,c], Shijie Liu [a,b], Can Wu [a,b], Yiqian Wang [a,b], Yubao Chen [a,b], Shaojun Lv [a,b], Fanglin Wang [a,b], Jingjing Meng [d], Gehui Wang [a,b,*]

[a] School of Geographic Sciences, Key Lab of Geographic Information Science of the Ministry of Education, East China Normal University, Shanghai 200241, China
[b] Institute of Eco-Chongming, 20 Cuiniao Rd., Chongming, Shanghai 202162, China
[c] Institute of Urban Meteorology, China Meteorological Administration, Beijing 100089, China
[d] School of Environment and Planning, Liaocheng University, Liaocheng 252000, China

HIGHLIGHTS

- Neutralization by NH_3 is the controlling factor for the efficient heterogeneous formation of sulfate.
- O_3 and NO_2 mixture shows a strong synergetic effect on the heterogeneous oxidation of SO_2 only under NH_3-rich conditions.
- The sharply rising ALWC caused by nitrate is responsible for the synergetic effect of mixed oxidants on sulfate formation.

GRAPHICAL ABSTRACT

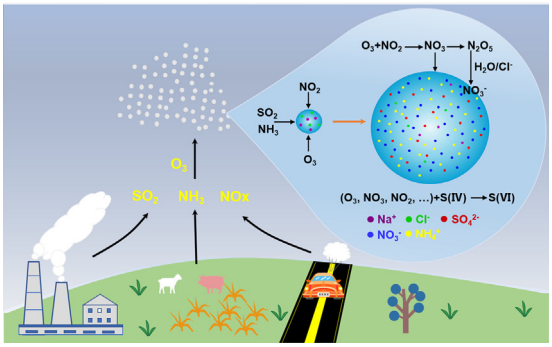

ARTICLE INFO

Article history:
Received 8 November 2020
Received in revised form 26 December 2020
Accepted 26 December 2020
Available online 29 January 2021

Editor: Pingqing Fu

Keywords:
Heterogeneous reaction
Ammonia neutralization
Sulfate and nitrate
Hygroscopic growth
Smog chamber simulation

ABSTRACT

Extremely high levels of atmospheric sulfate aerosols have still frequently occurred in China especially in winter haze periods and often been underestimated by models due to some missing formation mechanisms. Here we investigated the heterogeneous reaction dynamics of SO_2 oxidation by the abundantly co-existing O_3 and NO_2 in the urban atmosphere of China by using a laboratory smog chamber simulation technique. Our results showed that with an increase of NH_3 concentrations from 0.05 ppm to 1.5 ppm, SO_2 oxidation by O_3 can be greatly promoted and lead to an exponential increase of diameter growth factor (GF) of particles in the chamber from 1.29 to 1.98 for NaCl seeds and from 1.20 to 1.60 for $(NH_4)_2SO_4$ seeds, along with an increasing uptake coefficient (γ) of SO_2 from 4.47×10^{-5} to 1.52×10^{-4} on NaCl seeds and from 2.32×10^{-5} to 5.74×10^{-5} on $(NH_4)_2SO_4$ seeds, respectively. The heterogeneous production of sulfate from oxidation of SO_2 under NH_3-rich conditions by O_3 and NO_2 mixture in the chamber was 2.0–3.5 times the sum of sulfate from SO_2 oxidations by O_3 and NO_2, suggesting a strongly synergetic effect of the mixed oxidants on the heterogeneous oxidation of SO_2, which can cause rapid formation of $(NH_4)_2SO_4$ and NH_4NO_3 and is responsible for the explosive growth of $PM_{2.5}$ in the winter haze period of China. Our chamber results further showed that such synergetic process is only efficient under NH_3-rich conditions, clearly indicating that the combined controls on O_3, NOx and NH_3 are necessary for further mitigating the $PM_{2.5}$ pollution in China.

* Corresponding author at: School of Geographic Sciences, Key Lab of Geographic Information Science of the Ministry of Education, East China Normal University, Shanghai 200241, China.
E-mail address: ghwang@geo.ecnu.edu.cn (G. Wang).

https://doi.org/10.1016/j.scitotenv.2020.144897
0048-9697/

1. Introduction

Sulfate is one of the most abundant particles in the atmosphere, which is mainly generated via a series of multiphase chemical reactions (Sun et al., 2019; Zhang et al., 2013) and plays important roles in the global changes in climate and environment. Although the relative contribution of nitrate to particle pollution in China has increased quickly in the past decade and dominated the mass concentration of $PM_{2.5}$ due to the decrease in SO_2 emissions, concentration of atmospheric sulfate in the country is still very high, especially in winter haze periods (Lin et al., 2020; Ma et al., 2020; Wang et al., 2018a; Xie et al., 2020). The explicit mechanisms for the explosive growth of fine particles ($PM_{2.5}$) in China during severe haze periods are still under debate, of which rapid formation of sulfate is one of the focus.

Extensive studies have explored the formation mechanisms of atmospheric sulfate aerosols. Oxidation processes of SO_2 by O_3 (Li et al., 2007), H_2O_2 (Warneck, 1999), NO_2 (Ge et al., 2019b; Wang et al., 2016) and the catalytic oxidation by transitional metals ion (Alexander et al., 2009) in cloud and aerosol droplets are thought to be the main sulfate formation pathways by model simulations and laboratory investigations. However, in comparison with the field measurements the sulfate predictions by models tend to be underestimated, suggesting there are some unknown mechanisms on the sulfate formation (Gao et al., 2016a; Gao et al., 2016b). The role of different oxidants in atmospheric sulfate formation process is dependent on the different environmental conditions such as aerosol liquid water content (ALWC), aqueous phase acidity and oxidant levels. For example, a Lagrangian trajectory model study showed that at an initial pH of 5.0, H_2O_2 contributed about 86% to the total oxidation of SO_2 in cloud, followed by O_3 (~13%). However, at pH of 6.5 conditions, 74% of sulfate in cloud was from the reaction of H_2O_2 with S(IV) and 25% from O_3 (Venkataraman et al., 2001). Recently, both model and laboratory investigations showed that the contribution of NO_2 to sulfate formation in China during haze events is more important than other pathways when aerosol pH is higher than 5.4, which is the dominant formation pathway of sulfate in the atmosphere over the major part of North China Plain (Tao et al., 2020; Wang et al., 2016). Based on the Atmospheric Composition-Climate Model, Unger et al. (Unger et al., 2006) found that a 20% increase of sulfate pollution would be driven by the increasing of O_3 from 35 to 60 ppb. A most recent study simulated by the WRF-Chem-AWAC model suggested that the spatio-temporal variability of aerosol pH, different chemical regimes, reactant concentrations and meteorological conditions all have influences on the sulfate formation (Tao et al., 2020).

Because of the promulgation of the Clean Air Action laws in 2013, $PM_{2.5}$ pollution in China has been significantly mitigated. Zhai et al. (2019) reported that the annual concentrations of $PM_{2.5}$ across China decreased by 30–50% over the period of 2012 to 2018. Such changes have resulted in an increase in oxidizing capacity of the Chinese urban atmosphere, which is characterized by the abundantly co-existing O_3 and NO_2 in the country (Li et al., 2019). Under favorable meteorological conditions, the co-occurrence of O_3 and NO_2 may promote the formation of secondary aerosols, initiating an explosive growth of $PM_{2.5}$ in Chinese megacities. For example, Wu et al. (2020b) observed that the pollution events with O_3 and NO_2 simultaneously exceeding 100 μg m^{-3} frequently occurred in Shanghai during the autumn of 2019 and was often accompanied with sharp increases of $PM_{2.5}$ concentrations (Wu et al., 2020b).

In order to improve our understanding on the strategies for a further mitigation on the fine particle pollution in China, here we investigated the dynamics of the heterogeneous formation process of sulfate via SO_2 oxidation by O_3 and NO_2 mixture by using a smog chamber technique. Our results showed a strongly synergetic effect of O_3 and NO_2 on sulfate formation, highlighting the importance of combining controls on the emissions of NOx and related precursors in the country.

2. Experimental section

2.1. Materials and methods

Simulation experiments in this study were performed in a 1.1 m^3 smog chamber, which is composed of a 5.6 mm thick acrylic outer shell and 0.13 mm Teflon inner bag (Fig. S1). The experimental details have been described elsewhere (Ge et al., 2019b; Wang et al., 2016). Here we only give a brief description as follows.

Zero air, produced by the Zero Air Supply (Model 111 and Model 1150, Thermo Scientific), was used as background gas in all the experiments. Many field observations reported that wintertime severe haze events in China frequently occurred with a relative humidity (RH) larger than 90% (Ge et al., 2019b; Wang et al., 2016; Wu et al., 2019). Thus, in this work we chose a RH of 90 ± 1% condition in the chamber to mimic the sulfate formation by introducing a humid vapor flow produced from zero air bubbling through ultrapure water (Milli Q, 18.2 MΩ, Millipore Ltd., USA). Seeded particles were generated by a single jet atomizer (7388SJA, TSI) from a bulk solution containing NaCl or $(NH_4)_2SO_4$. Then, the seeded aerosols were dried by passing through two tandem Nafion dryers. Afterwards, the aerosol particles with a diameter of 100 nm were selected by a Differential Mobility Analyzer (DMA) and introduced into the chamber. The initial concentration of the selected seeds in the chamber was about 5×10^4 cm^{-3}. The reactant gases including SO_2, NO_2, and NH_3 were purchased from Air Liquide Holding Co., Ltd. (China) and were injected individually into the chamber using a glass syringe. Ozone was generated by an ozonizer (LT-100, China) via ionizing high purity oxygen (99.999%) and introduced into the chamber directly. All the experiments in this work were conducted at 298 K (room temperature) and 1 atm.

2.2. Monitoring analysis

Reactant gases (SO_2, NOx, O_3) in the chamber were monitored by Thermos scientific analyzers (SO_2, NOx, O_3 analyzers), respectively. The Scanning Mobility Particle Sizer (SMPS, model 3082) was used to measure the size parameters of aerosols including size distribution, number and mass concentrations. The chemical compositions of the particles in the chamber were analyzed by a high-resolution time-of-flight aerosol mass spectrometer (HR-ToF-AMS, Aerodyne Company, USA).

2.3. Smog chamber experiments

To investigate the synergistic oxidation effect of O_3 and NO_2 on sulfate formation in the urban atmosphere of China during the haze development process, experiments about SO_2 oxidation by O_3 or/and NO_2 were conducted. In the current work, NaCl and $(NH_4)_2SO_4$ were chosen as seeds. The initial conditions of the simulation experiments are listed in Table S1.

The aims of experiments 1–10 were to compare the effects of different seed particles on sulfate formation via SO_2 oxidation by O_3, and the role of varied concentrations of NH_3 in sulfate formation during this process were further studied. As control experiments, the experiments of SO_2 oxidized by NO_2 (exp. 11–12) were conducted based on our previous work (Ge et al., 2019b). The process of SO_2 oxidation by mixed oxidants (O_3 + NO_2) with 1 ppm NH_3 in the presence of NaCl or $(NH_4)_2SO_4$ seed particles were studied by exp.13–16. To mimic the meteorological conditions of severe haze in China that are characteristic of very weak solar radiation due to high RH conditions and heavy particle pollution, all the chamber experiments in this work were performed under RH of 90 ± 1% and dark conditions by using an anti-UV cloth hood covering the chamber.

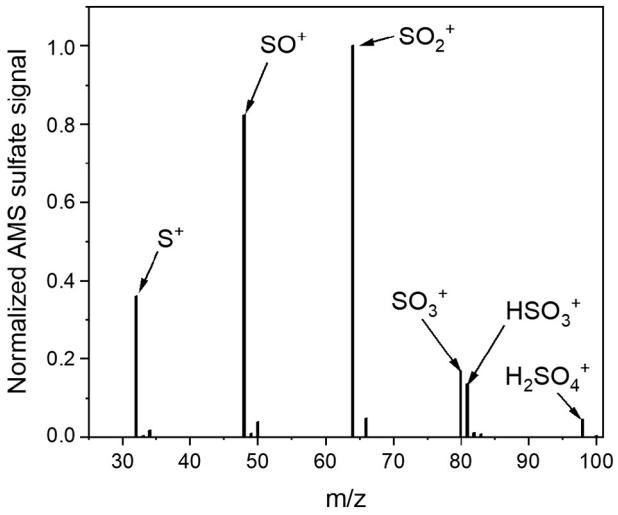

Fig. 1. HR-ToF-AMS spectra of sulfate ions of particles in the $SO_2/O_3/NH_3$/NaCl system (Note: water and ammonium ions are excluded).

3. Results

3.1. Effects of NH_3 on SO_2 oxidation by O_3

Heterogeneous oxidation of SO_2 by O_3 in wet aerosols is one of the major formation pathways of atmospheric sulfate in the planetary boundary layer, such an aqueous phase oxidation is highly pH dependent (Reilly et al., 2001) and thus can be significantly promoted under NH_3-rich conditions. To quantitatively investigate the promoting effects of NH_3 on the heterogeneous SO_2 oxidation by O_3, NaCl and $(NH_4)_2SO_4$ seeds, which are two common particles in the urban atmosphere of China (Ding et al., 2020; Wang et al., 2014; Wang et al., 2013), were exposed to SO_2 and O_3 for about 2 h, respectively, and measured for chemical composition by HR-ToF-AMS and size distribution by SMPS. As shown in Fig. 1, strong signals of fragment ions (m/z = 96, 81, 80, 64, 48 and 32) were detected after the exposure of the seeded NaCl particles to SO_2 in the presence of O_3, demonstrating that SO_4^{2-} was the product of the reaction of SO_2 with O_3. As seen in Fig. 2a, mass concentration of particles in the chamber during Phase I kept constant after exposing NaCl seeds to SO_2 for about 30 min and no any signal of sulfur-containing ions was observed by the HR-ToF-AMS, suggesting that no detectable amount of sulfate or sulfite was formed via the reaction of SO_2 with the background gas ($O_2 + N_2$) on the seeds or hydrolysis of SO_2 in the aerosol aqueous phase under the 90 ± 1% RH conditions (Fig. 2a, Phase I). When O_3 was introduced into the chamber, the mass concentration of particles increased by 4.05 ± 1.19 μg m^{-3} in the SO_2/O_3/NaCl system, and the dry diameter of particles in the chamber grew from 101.8 nm to 126.3 nm (Fig. 2a, Phase II), which was due to the formation of H_2SO_4 on the aerosol aqueous phase through oxidation of SO_2 by O_3. A similar phenomenon was also observed for the $SO_2/O_3/(NH_4)_2SO_4$ system (Fig. 2b, Phase I and Phase II), in which concentration of particles in the chamber increased by 2.83 ± 0.60 μg m^{-3} and the corresponding size of the seeded $(NH_4)_2SO_4$ particles increased from 101.8 nm to 117.6 nm in a dry diameter. Such an increase in particle size in the absence of NH_3 was not observed by our previous studies (Ge et al., 2019b; Wang et al., 2016), which exposed the two types of seeds to SO_2 and NO_2 under the same experiment conditions, indicating that the oxidizing ability of O_3 to SO_2 is stronger than that of NO_2.

A significant increase of particle concentration was observed when NH_3 was subsequently introduced into the chamber (Fig. 2a, Phase III). When the concentration of NH_3 in the chamber varied from 0.05–1.5 ppm, the increase in concentration of particles varied from 8.93 μg m^{-3} to 55.58 μg m^{-3} for the NaCl seeds, which was 2.2 to 13.6 times higher than that in the absence of NH_3 (Fig. 2a, Phase II). The formed H_2SO_4 was neutralized by NH_3 into $(NH_4)_2SO_4$, which could decrease aerosol acidity and thus promoted the heterogeneous oxidation of SO_2 by O_3. As for the $(NH_4)_2SO_4$ seeds, when NH_3 increased from 0.5 ppm to 1.5 ppm, the increase in concentration of particles in the chamber varied from 3.71 μg m^{-3} to18.61 μg m^{-3} (Fig. 2b, Phase III), which is 1.3–6.6 times higher than that in the Phase II period (Fig. 2b, Phase II).

Fig. 3 shows the growth factor (GF) of particles in the chamber as a function of NH_3 levels. The GF of both NaCl and $(NH_4)_2SO_4$ seeds showed an exponential increase with an increase of NH_3 levels, suggesting the promoting effect of NH_3 on the sulfate formation. The GF of NaCl seeds is about 10–30% larger than that of $(NH_4)_2SO_4$ seeds, indicating the more efficient production of sulfate with NaCl seeds compared to $(NH_4)_2SO_4$ seeds. At 90 ± 1% RH conditions the hygroscopic growth factor of 100 nm NaCl particles is 2.3 and larger than that (1.48) of 100 nm $(NH_4)_2SO_4$ particles. We used the ISORROPIA-II thermodynamic model to further calculate the hygroscopicity of seeded particles in our chamber. The results showed that at 90% RH conditions the aerosol liquid water content of per mass of particles (ALWC/mass) in the chamber is 9.7 for the NaCl seeds and 3.09 for the $(NH_4)_2SO_4$ particles, suggesting that NaCl is more hygroscopic and its higher ALWC is favorable for the

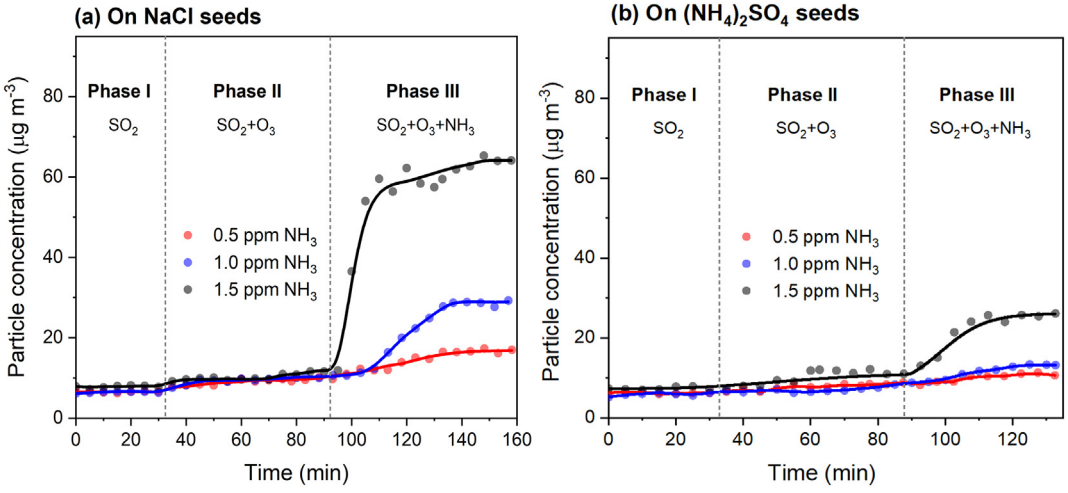

Fig. 2. Variations in mass concentration of particles in the chamber during the successive exposures of the seeds to SO_2, O_3 and NH_3 ((a) NaCl seeds with a 100 nm diameter and (b) $(NH_4)_2SO_4$ seeds with a 100 nm diameter).

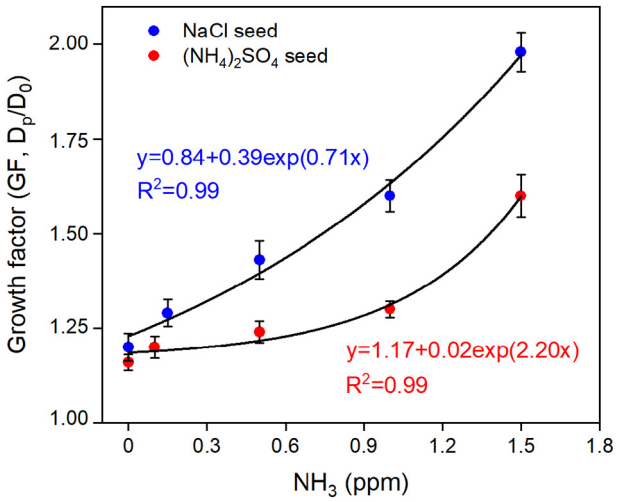

Fig. 3. The growth factor of seeded particles in the chamber as a function of NH_3 levels after the exposure to O_3 (0.6 ppm) and SO_2 (0.7 ppm) for 2.5 h at 90 ± 1% RH conditions (D_0 and D_p are the dry diameters of particles in the chamber before and after the exposure, respectively).

heterogeneous formation of sulfate (Badger et al., 2006; Peng et al., 2016). Besides, another proposed chemistry mechanism in NaCl aqueous phase has been elucidated that O_3 can react with Cl^- on the surface to form OH^- (Faxon and Allen, 2013; Keene et al., 1990; Li et al., 2007). The alkaline surface can greatly promote the hydrolysis of SO_2. In contrast, the weakly acidic $(NH_4)_2SO_4$ could be unfavorable to the hydrolysis of SO_2 in liquid phase (Wang et al., 2018a). Therefore, heterogeneous oxidation of SO_2 by O_3 proceeded more efficiently on the NaCl seeds.

Based on the particle compositions measured by HR-ToF-AMS, the pH value and ALWC of particles in the chamber at the end of the experiments were calculated by using the ISORROPIA II thermodynamic equilibrium model with the assumption of aerosol in metastable state (Wang et al., 2018a). The acidity of neutral NaCl seeds sharply decreased from pH = 7 to pH = 0.7 when NaCl seeds were exposed to 0.7 ppm SO_2 in the absence of NH_3. Researchers have verified that NH_3 plays an effective role in particle formation with sulfuric acid because of their basicity (Benson et al., 2009; Chen et al., 2018a; Chen et al., 2016; DePalma et al., 2014; Lehtipalo et al., 2016; Qiu et al., 2011; Qiu and Zhang, 2013). With the neutralization of NH_3, the acidity of particles decreased and was favorable for sulfate formation sustainably in the acidified NaCl droplets. NH_3 could decrease aerosol acidity effectively, varied from pH = 4.5 in experiments with 0.05 ppm NH_3 to pH = 5.6 with 1.0 ppm NH_3 for the $SO_2/O_3/NH_3$/NaCl system (Fig. 4a). Similar increasing pH trend was also observed for $(NH_4)_2SO_4$ seeds, of which the pH of aerosols changed from 3.6 under 0.1 ppm NH_3 to 4.8 under 1.5 ppm NH_3 (Fig. 4b).

The reactive uptake coefficients (γ) of SO_2 on the two types of seeded particles with various concentrations of NH_3 can be calculated based on the following Eq. (E1):

$$\frac{d[sulfate]}{dt} = k[SO_2(g)] = \frac{1}{4}\gamma \bar{C} S[SO_2(g)] \quad \text{(E1)}$$

where [*sulfate*] is the molar concentration of sulfate produced during *t* reaction time period, γ is the uptake coefficient of SO_2, $\bar{C}$ is the mean molecular speed, *S* is the aerosol surface area, and $[SO_2(g)]$ is SO_2 concentration in the gas phase. As shown in Table 1, in the $SO_2/O_3/NH_3$/NaCl system, the γ of SO_2 for sulfate formation under different NH_3 levels (0.05–1.5 ppm) was in the range of 4.47×10^{-5}–1.52×10^{-4}, while the γ was in the range of 2.32×10^{-5}–5.74×10^{-5} in the $SO_2/O_3/NH_3/(NH_4)_2SO_4$ system, suggesting that the uptake of SO_2 on both NaCl and $(NH_4)_2SO_4$ seeds increased with increasing concentrations of NH_3. Thus, more NH_3 could promote the formation rate of sulfate in the atmosphere.

3.2. Synergistic effects of O_3 and NO_2 on sulfate formation under NH_3-rich conditions

To explore the synergetic effect of mixed oxidants of O_3 and NO_2 on sulfate formation, experiments with NO_2 introduced into the chamber were further conducted based on the process of SO_2 oxidation by O_3. Fig. 5 shows the temporal variations in dry diameter and composition of particles in the chamber. The experimental results showed that particle sizes further increased after introducing NO_2, and a more obvious increase can be obtained when NH_3 was introduced into the chamber based on the reactions of SO_2 with O_3. Due to the reactions of SO_2 with O_3, the mean diameter of NaCl particles grew from 117.6 nm to 145.9 nm (Fig. 5a, Phase I). When 0.3 ppm NO_2 was subsequently introduced into the chamber, the mean diameter of particles grew dramatically to 259.5 nm (Fig. 5a, Phase II). A further shift of particle diameter to 371.8 nm was observed when 1.0 ppm NH_3 was introduced into the chamber (Fig. 5a, Phase III). A similar increasing pattern of particle sizes was also observed for the seeded $(NH_4)_2SO_4$ particles, which

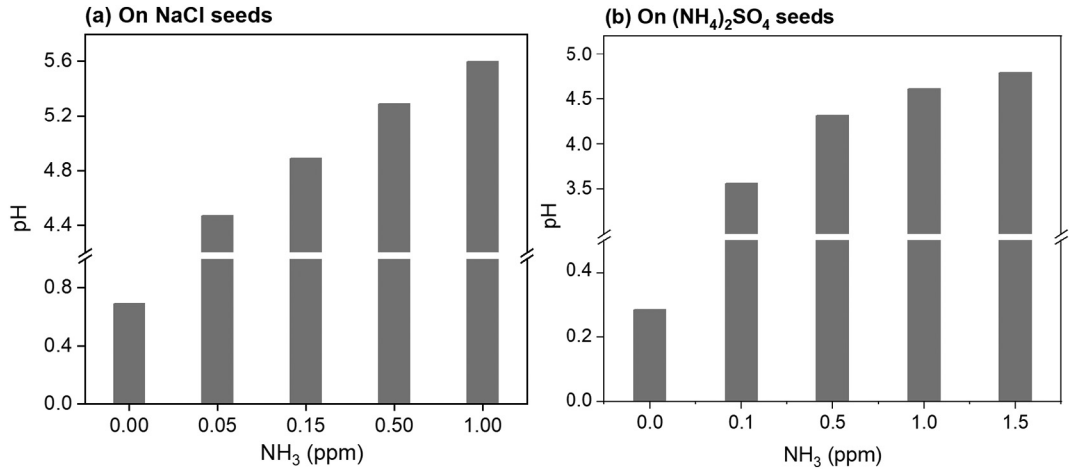

Fig. 4. pH values of particles in the chamber with different NH_3 concentrations after the exposures of (a) NaCl seeds and (b) $(NH_4)_2SO_4$ seeds to SO_2 (0.7 ppm) and O_3 (0.6 ppm) under 90 ± 1% RH conditions for 2.5 h.

Table 1
Uptake coefficients of SO_2 under different NH_3 concentrations in the $SO_2/O_3/NH_3$/seed systems.

Seed	NH_3 (ppm)	Growth in SO_4^{2-} ($\mu g\ m^{-3}$)	Surface area[a] ($cm^2\ cm^{-3}$)	γ
NaCl	0.05	8.93	3.38×10^{-6}	4.47×10^{-5}
(D_0 = 100 nm)	0.15	6.46	1.51×10^{-6}	6.98×10^{-5}
	0.30	9.46	2.28×10^{-6}	7.23×10^{-5}
	0.50	10.30	1.89×10^{-6}	9.15×10^{-5}
	1.0	22.58	3.48×10^{-6}	1.10×10^{-4}
	1.5	55.58	6.23×10^{-6}	1.52×10^{-4}
$(NH_4)_2SO_4$	0.1	3.71	2.22×10^{-6}	2.32×10^{-5}
(D_0 = 100 nm)	0.5	4.77	2.27×10^{-6}	2.84×10^{-5}
	1.0	6.70	2.33×10^{-6}	4.08×10^{-5}
	1.5	18.61	4.54×10^{-6}	5.74×10^{-5}

[a] Surface area is the surface area of particles in the chamber during the exposure.

increased from 121.9 nm to 140.7 nm after the reactions of SO_2 with O_3 (Fig. 5c, Phase I), then grew sharply to 259.5 nm after introducing NO_2 into the chamber (Fig. 5c, Phase II), and further shifted to 333.8 nm in the presence of 1.0 ppm NH_3 (Fig. 5c, Phase III).

As shown in Fig. 5b, there was 10.28 $\mu g\ m^{-3}$ of SO_4^{2-} formed in the Phase I period due to the reactions of SO_2 with O_3 on the wetted NaCl seed surface. When NO_2 was subsequently introduced into the chamber, abundant NO_3^- (99.83 $\mu g\ m^{-3}$) (Fig. 5a and b, Phase II) was generated but concentration of SO_4^{2-} was almost entirely equal to that in Phase I. Since no NH_3 was introduced in the two stages, SO_4^{2-} and NO_3^- on the seeded particles in Phase I and Phase II mainly existed as H_2SO_4 and HNO_3, respectively, and the particle growth was caused by the accumulation of both acids on the seeds (Fig. 5b, Phase I and Phase II). After introducing 1.0 ppm NH_3 into the chamber, sharply increased concentrations of SO_4^{2-} (44.07 $\mu g\ m^{-3}$, Fig. 5b), NO_3^- (233.81 $\mu g\ m^{-3}$) and NH_4^+ (67.93 $\mu g\ m^{-3}$) were observed, leading to a rapid growth in the diameter of seeded particles (Fig. 5a, Phase III). Abundant SO_4^{2-}, NO_3^- and NH_4^+ were also observed in the experiments with $(NH_4)_2SO_4$ as the seeds, which were 17.05 $\mu g\ m^{-3}$, 131.95 $\mu g\ m^{-3}$, and 36.37 $\mu g\ m^{-3}$ under the 1.0 ppm NH_3 conditions, respectively (Fig. 5c and d). O_3 in the chamber can react with NO_2 and form N_2O_5, which is highly reactive and can quickly be hydrolyzed into HNO_3 on the hygroscopic surface (Chen et al., 2018b; McDuffie et al., 2018). Gaston et al. reported that reactive uptake is the main pathway for N_2O_5 diffused into $(NH_4)_2SO_4$ droplets to form HNO_3. However, a near-surface reaction between absorbed N_2O_5 with Cl^- in NaCl droplets dominated the uptake of N_2O_5, which is much faster than the diffusion process of N_2O_5 with H_2O (Gaston and Thornton, 2016). Thus, more nitrate can be formed on NaCl seeds than on $(NH_4)_2SO_4$ seeds. The formed NH_4NO_3 can absorb more water vapor and in turn further promote the heterogeneous formation of $(NH_4)_2SO_4$ and NH_4NO_3 (Phase III in Fig. 5b and d, respectively).

As shown in Fig. 5, O_3 and NO_2 did not show synergistic effects on sulfate formation in the absence of NH_3, although HNO_3 could be formed via the reaction of O_3 with NO_2. Our previous work found that SO_2 oxidation by NO_2 cannot proceed efficiently under NH_3-poor conditions (Ge et al., 2019b; Wang et al., 2018a; Wang et al., 2016), because SO_2 is a weak acid and the formed H_2SO_4 could prevent SO_2 from dissolving into the acid solution. However, as seen in Fig. 5, O_3 and NO_2 showed a strong synergetic effect on sulfate formation in the presence of NH_3 in the chamber. Under the experiment conditions with NaCl as the seeds, the amount of sulfate (44.07 $\mu g\ m^{-3}$) formed by the mixed oxidants of O_3 and NO_2 was 2.7 and 8.2 times higher than the amount of sulfate formed by the oxidation of O_3 or NO_2 alone in the presence of NH_3, which was 16.42 $\mu g\ m^{-3}$ and 5.36 $\mu g\ m^{-3}$, respectively (Table 2). Similar increased sulfate formation was also observed for the experiments with $(NH_4)_2SO_4$ as the seeds, clearly demonstrating a strong synergetic effect of the mixed O_3 and NO_2 on sulfate formation, which is effective only under NH_3-rich conditions (Fig. 5, Phase III).

The uptake coefficients of SO_2 on NaCl or $(NH_4)_2SO_4$ seeds in experiments with mixed oxidants of O_3 and NO_2 in the presence of 1.0 ppm NH_3 were further calculated. As seen in Table 3, the value of γ on NaCl seeds was 9.25×10^{-5}, and 4.24×10^{-5} on $(NH_4)_2SO_4$ seeds, respectively, which is close to that in the experiments with O_3 as the oxidant. Due to the formation of sulfate, nitrate, and ammonium on the seeded particles and the subsequent absorption of water vapor, the surface area of aerosols in the chamber rapidly increased. As shown by the

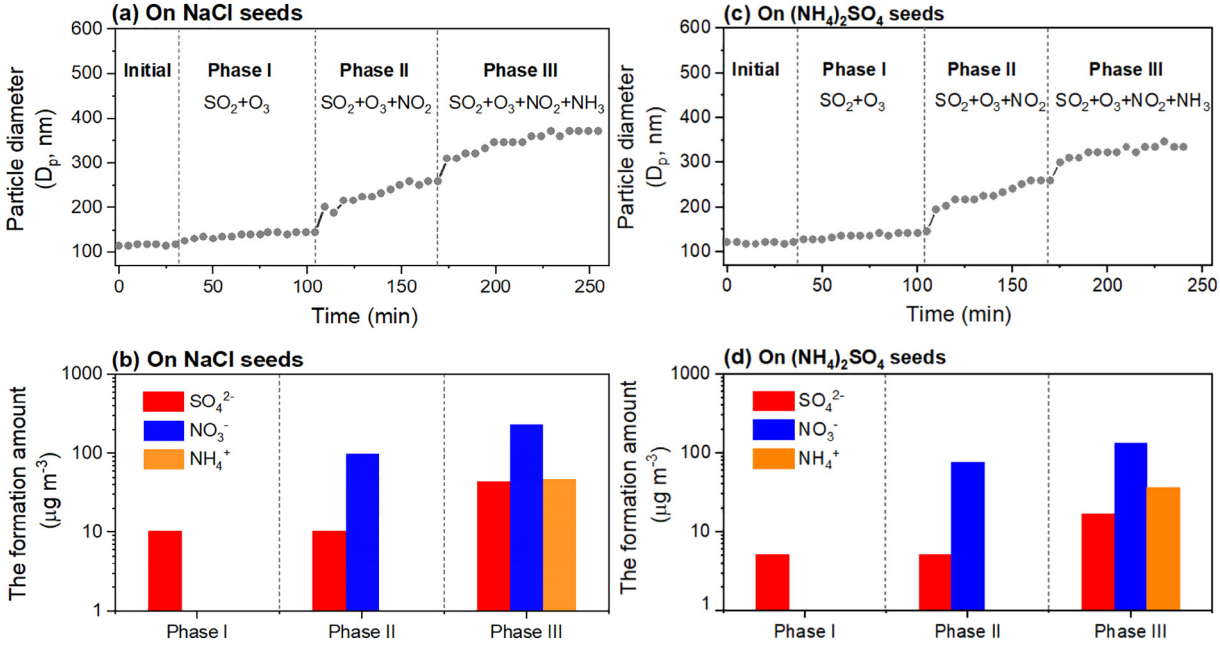

Fig. 5. Evolution of size and composition of particles in the chamber (Initial concentrations of SO_2, O_3, NO_2, NH_3 in the chamber were 0.8 ppm, 0.3 ppm, 0.3 ppm, 1.0 ppm, respectively) ((a) mean diameter of the seeded NaCl particles, (b) sulfate, nitrate and ammonium secondarily formed in the chamber after exposing NaCl seeds to the gaseous reactants, (c) mean diameter of the seeded $(NH_4)_2SO_4$ particles, and (d) sulfate, nitrate and ammonium secondarily formed in the chamber after exposing $(NH_4)_2SO_4$ seeds to the gaseous reactants).

Table 2
Concentrations of SO_4^{2-}, NO_3^- and NH_4^+ formed in the chamber after the exposure of NaCl or $(NH_4)_2SO_4$ seeds to different oxidants for about 2.5 h in the presence of NH_3.

Oxidant	Seed[a]	RH (%)	SO_2 (ppm)	NH_3 (ppm)	ΔSO_4^{2-}[a] ($\mu g\ m^{-3}$)	ΔNO_3^-[a]	ΔNH_4^+[a]
O_3 (0.7 ppm)	NaCl	90 ± 1	0.8	1.0	16.42	0.0	6.2
NO_2 (0.6 ppm)		90 ± 1	0.8	1.0	5.36	0.0	2.0
NO_2 + O_3 (0.3 ppm + 0.3 ppm)		90 ± 1	0.8	1.0	44.07	234	68
O_3 (0.7 ppm)	$(NH_4)_2SO_4$	90 ± 1	0.8	1.0	4.87	0.0	1.8
NO_2 (0.6 ppm)		90 ± 1	0.8	1.0	0.0	0.0	0.37
NO_2 + O_3 (0.3 ppm + 0.3 ppm)		90 ± 1	0.8	1.0	17.05	132	36

[a] ΔSO_4^{2-}, ΔNO_3^- and ΔNH_4^+ are the difference in the concentrations before and after the exposures.

Eq. (E1), the aerosol surface area is inversely correlated with the uptake coefficient γ. Thus, the γ for the mixed oxidants was not obviously greater than that for the single oxidant under the same experimental conditions.

4. Discussion

4.1. Reaction mechanisms for SO_2 oxidation by the mixed oxidants of O_3 and NO_2 under NH_3-rich conditions

In the atmosphere sulfate is mainly formed by aqueous phase reactions of SO_2 with O_3, NO_2, H_2O_2, OH radicals, and transitional metal ion catalysis (Cheng et al., 2016; Ma et al., 2013; Park et al., 2017; Wang et al., 2016). In the urban atmosphere, the heterogeneous oxidation of SO_2 by O_3 or NO_2 follows the reaction pathways of (R1)–(R3) (Ge et al., 2019b; Li et al., 2007), among which the dominant role of NO_2 on sulfate formation in the winter haze period of China was firstly pointed out by Wang et al. in 2016 (Wang et al., 2016), based on their field measurements and smog chamber simulation, and recently recognized by the atmospheric aerosol community with an increasing number of publications (Cheng et al., 2016; Tao et al., 2020; Wang et al., 2020; Xue et al., 2019). For example, by combing the field observation and numerical simulation, Tao et al. (Tao et al., 2020) found that SO_2 oxidation by NO_2 is the dominant pathway for sulfate formation in the megacity region of Beijing and the large area of Hebei Province, China.

$$SO_2\ (g) + H_2O\ (aq) + NH_3(g) \rightarrow HSO_3^-(aq) + NH_4^+(aq) \quad (R1)$$

$$HSO_3^-(aq) + O_3(aq) \rightarrow HSO_4^-(aq) + O_2(g) \quad (R2)$$

$$HSO_3^-(aq) + NO_2(aq) \rightarrow SO_4^{2-}(aq) + HONO(g) \quad (R3)$$

A few field investigations have shown that O_3, NO_2 and NH_3, as well as VOCs in the urban atmosphere of China are abundantly co-existing (Vu et al., 2019; Zheng et al., 2018). Through this study, we found that the heterogeneous oxidation of SO_2 by the mixture of O_3 and NO_2 to produce sulfate was much more efficient than by them single alone under NH_3-rich conditions. The synergistic effects of mixed O_3 and NO_2 on sulfate formation include a series of reaction processes as follows.

Firstly, besides the direct oxidation of SO_2 by O_3 and NO_2, respectively, O_3 and NO_2 in the atmosphere can react with each other, and NO_3, a highly reactive gas, would be generated during this process. The formed NO_3 can further react with NO_2 to form N_2O_5 ((R4)–(R5)),

Table 3
The uptake coefficient (γ) of SO_2 during the exposure of the 100 nm diameter of seeds to the mixed NO_2 (0.3 ppm) and O_3 (0.3 ppm) oxidant under 90 ± 1% RH conditions.

Seed	NH_3 (ppm)	ΔSO_4^{2-}[a] ($\mu g\ m^{-3}$)	Surface area of particles ($cm^2\ cm^{-3}$)	γ
NaCl	1.0	60.60	8.56×10^{-6}	9.25×10^{-5}
$(NH_4)_2SO_4$	1.0	23.44	7.57×10^{-6}	4.24×10^{-5}

[a] ΔSO_4^{2-} is the difference of the sulfate concentration before and after the exposures.

which is the main source of nitrate at night (R6) (Liebmann et al., 2019; Wang et al., 2018b). During the process of heterogeneous reactions in the two SO_2/(O_3 + NO_2)/NH_3/seed systems, the quicker generation rate of nitrate leaded to massive nitrate formed, which was about one order of magnitude higher than sulfate before NH_3 was introduced (Fig. 5, Phase II). The existence of NH_3 can neutralize the acidity of particles, favoring more dissolution of acidic NO_2 and SO_2 (Yang et al., 2018). For example, in the experiments with NaCl seeds, the amount of nitrate increased from 99.83 $\mu g\ m^{-3}$ without NH_3 to 233.81 $\mu g\ m^{-3}$ in the presence of NH_3. The strong hygroscopicity of nitrate can greatly enhance ALWC of particles in the chamber. In this work, the ALWC caused by nitrate formed in the chamber under the 1.0 ppm NH_3 and 90 ± 1% RH conditions was 1049 $\mu g\ m^{-3}$ for the NaCl seeds and 956 $\mu g\ m^{-3}$ for the $(NH_4)_2SO_4$ seeds, respectively, which is about ten times higher than that under the oxidation by O_3 or NO_2 alone. Thus, the enhanced ALWC in aerosol particles by large amount of nitrate via the reactions of O_3 and NO_2 provides a favorable environment for sulfate formation in the SO_2/O_3/NO_2/NH_3/seed system (Ge et al., 2019a).

$$NO_2(g) + O_3(g) \rightarrow NO_3(g) + O_2(g) \quad (R4)$$

$$NO_3(g) + NO_2(g) \rightleftharpoons N_2O_5(g) \quad (R5)$$

$$N_2O_5(g) + (H_2O \text{ or } Cl^-)(aq) \rightarrow NO_3^-(aq) + ClNO_2(g) \quad (R6)$$

Secondly, NO_3 is also an important oxidant product during the reaction process of NO_2 with O_3 (Brown and Stutz, 2012). Previous work had proposed that NO_3 could enhance sulfate production via the series of reactions of (R7)–(R10) (Chameides, 1986; Feingold, 2002). Rudich et al. (1998) found that in polluted areas where high concentrations of dissolved S(IV) was present in the droplets, the role of NO_3 in sulfate formation accounted for significant oxidation in the marine boundary layer; their simulation results showed that the relative contribution to sulfate by the uptake of 2.5 ppt NO_3 accounted for about 50% of the sulfate formation by 40 ppb of O_3 in 30 min (Rudich et al., 1998). These results suggest that S(IV) oxidation by NO_3 probably also contributed to the synergetic effect observed by this work (Chameides, 1986; Hung and Hoffmann, 2015).

$$HSO_3^-\ (aq) + NO_3\ (aq) \rightarrow NO_3^-\ (aq) + H^+(aq) + SO_3^-(aq) \quad (R7)$$

$$SO_3^-\ (aq) + O_2\ (aq) \rightarrow SO_5^-\ (aq) \quad (R8)$$

$$HSO_3^-(aq) + SO_5^-\ (aq) \rightarrow H^+(aq) + SO_4^{2-}(aq) + SO_4^-(aq) \quad (R9)$$

$$HSO_3^-(aq) + SO_4^-\ (aq) \rightarrow H^+(aq) + SO_4^{2-}(aq) + SO_3^-(aq) \quad (R10)$$

Thirdly, as seeds, NaCl particles are of greater effects on nitrate and sulfate formation than that of $(NH_4)_2SO_4$ seeds. One of the reasons for this phenomenon is that NaCl has a stronger hygroscopicity ability than $(NH_4)_2SO_4$ under the similar conditions (Hu et al., 2010; Park et al., 2008). Moreover, chloride ions in the NaCl droplets can react with O_3 and NO_3, and the products during these processes may affect the oxidation of S(IV). Early researches have explored these reaction mechanisms and found that Cl_2 could be produced during the process.

For example, using a chemical ionization mass spectrometer, Abbatt and Waschewsky (1998) observed an increase in the signal of Cl_2 with a decline in the ozone signal in a flow tube study of heterogeneous reactions of O_3 with NaCl aerosols (Abbatt and Waschewsky, 1998). Keene et al. (1990) used O—D photochemical model simulations of the marine surface air sampled to investigate the geochemical cycling of reactive Cl, and reported an accumulation of Cl_2 during the night from the O_3 reaction at NaCl surface (Keene et al., 1990). For reactions of chloride ions with NO_3 radical, the formation of nitrate ions was observed by Schütze and Herrmann (2005) in a single drop experiment of the uptake of NO_3 radical on NaCl solution (Schütze and Herrmann, 2005). Several researches further pointed out that O_3 can react with Cl^- to generate an alkaline surface on the NaCl particle surface (R11), which can promote the hydrolysis of SO_2 in the aqueous surface of aerosols (Faxon and Allen, 2013; Laskin et al., 2003; Li et al., 2007). The formed NO_3 by reaction of O_3 with NO_2 can react with Cl^- to form Cl radical and Cl_2^- via a series of reactions ((R12)–(R13)). Both Cl_2^- and Cl radical can further oxidize HSO_3^- into sulfate ((R14)–(R15)) (Chameides, 1986; Hung and Hoffmann, 2015). Thus, in addition to the stronger hygroscopicity, the factors mentioned above may be also responsible for the stronger promoting effect of NaCl seeds on sulfate formation than that of $(NH_4)_2SO_4$ seeds observed by the current chamber experiments.

$$O_3\,(aq) + H_2O\,(aq) + Cl^-(aq) \rightarrow 2OH^-(aq) + Cl_2(g) + O_2(g) \quad (R11)$$

$$NO_3(aq) + Cl^-(aq) \rightarrow NO_3{}^-(aq) + Cl(aq) \quad (R12)$$

$$Cl(aq) + Cl^-(aq) \rightleftharpoons Cl_2{}^-\,(aq) \quad (R13)$$

$$HSO_3{}^-(aq) + Cl_2{}^-\,(aq) \rightarrow 2Cl^-\,(aq) + H^+(aq) + SO_3{}^-(aq) \quad (R14)$$

$$HSO_3{}^-(aq) + Cl\,(aq) \rightarrow Cl^-\,(aq) + H^+(aq) + SO_3{}^-(aq) \quad (R15)$$

In conclusion, the detailed chemical mechanisms for the synergetic effects of mixed O_3 and NO_2 on sulfate formation are very complicated. However, the role of NH_3 observed in this work suggested that an enhanced hygroscopicity of aerosols due to the fast formation of NH_4NO_3 by the reaction of O_3 with NO_2 and the subsequent absorption of water vapor could be the main reason, which significantly promoted the dissolution of all the reactants into the aerosol aqueous phase, enhancing the productions of sulfate and nitrate, as schematically plotted in Fig. 6.

4.2. Implications for the haze formation in China

Sulfate is still one of the major components of $PM_{2.5}$ in China especially during winter haze periods, although SO_2 emission has been decreasing significantly in the past years (Ge et al., 2019b; Wu et al., 2020a; Xie et al., 2020). An explosive growth of $PM_{2.5}$ that is dominated by $(NH_4)_2SO_4$ and NH_4NO_3 has still frequently occurred in Beijing, Shanghai and many other cities in China. However, the sharp increase in sulfate and nitrate concentrations during the Chinese haze development is often underestimated by current models especially for sulfate because of the lack of dynamic descriptions that can accurately track the aqueous phase formation process of sulfate in the country (Gao et al., 2016b). Concentrations of $PM_{2.5}$ and sulfate in China have decreased significantly since 2013, because Chinese government has promulgated very strict controls on the emission of SO_2 and smokes from coal-burning power plants in the country. However, due to the rapid increases in vehicle numbers, NOx and VOC levels in China are still very high. Zhai et al. (2019) and Zhang et al. (2019) reported that compared to 2013, air pollutant levels across China in 2018 have decreased by 30–50% for $PM_{2.5}$ and by 57–76% for SO_2 but NOx has decreased only by 21% in 2017 while VOC and NH_3 emissions have kept constant and even slightly increased. The abundant co-occurrence of NOx and VOC is favorable for photochemical reaction, resulting in high levels of O_3 and NO_2 in many regions of China such as Beijing and Shanghai (Li et al., 2019).

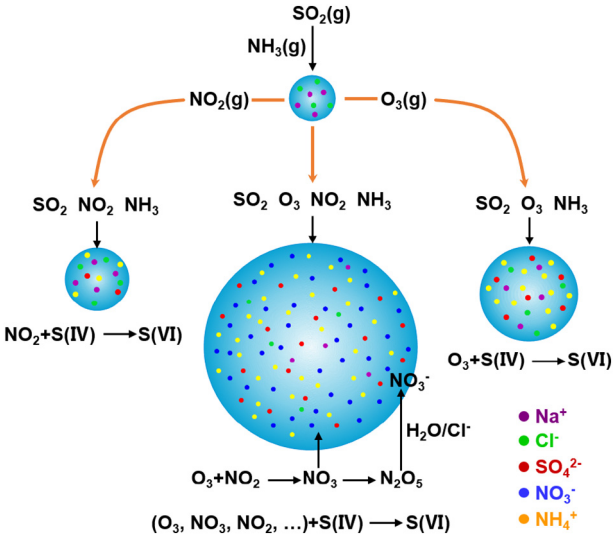

Fig. 6. A schematic plot for the heterogeneous formation mechanism of sulfate from the synergetic oxidation of SO_2 by NO_2 and O_3.

Based on the lab chamber simulation, this work has revealed a strongly synergetic effect of O_3 and NO_2 on sulfate formation, which can efficiently proceed under NH_3-rich conditions and lead to the rapid formation of hygroscopic secondary $(NH_4)_2SO_4$ and NH_4NO_3 aerosols in the haze periods of China. Our work suggested that combined measures to simultaneously control O_3, NO_2 and NH_3 emissions in China are necessary for a further mitigation of haze pollution in the country.

CRediT authorship contribution statement

GW conceived the experiment. SZ, DL and SG performed the experiment. GW, SZ and SG conducted the data interpretation and wrote the paper. SL, YW, CW, SL, FW and YC contributed useful discussions and comments.

Declaration of competing interest

We declare that we have no known competing financial interests or personal relationships that could have appeared to influence the work reported in this paper.

Acknowledgements

This work was financially supported by the National Key Research and Development Plan programs (No. 2017YFC0210000 and 2017YFC0212703), Natural Science Foundation of China (No. 41773117 and 41807355), the programs from Institute of Eco-Chongming and ECNU Happiness Flower.

Appendix A. Supplementary data

Supplementary data to this article can be found online at https://doi.org/10.1016/j.scitotenv.2020.144897.

References

Abbatt, J.P.D., Waschewsky, G.C.G., 1998. Heterogeneous interactions of HOBr, HNO_3, O_3, and NO_2 with deliquescent NaCl aerosols at room temperature. J. Phys. Chem. A 102, 3719–3725.

Alexander, B., Park, R.J., Jacob, D.J., Gong, S., 2009. Transition metal-catalyzed oxidation of atmospheric sulfur: global implications for the sulfur budget. J. Geophys. Res. 114, D02309.

Badger, C.L., George, I., Griffiths, P.T., Braban, C.F., Cox, R.A., Abbatt, J.P.D., 2006. Phase transitions and hygroscopic growth of aerosol particles containing humic acid and mixtures of humic acid and ammonium sulphate. Atmos. Chem. Phys. 6, 755–768.
Benson, D.R., Erupe, M.E., Lee, S.H., 2009. Laboratory-measured H_2SO_4-H_2O-NH_3 ternary homogeneous nucleation rates: initial observations. Geophys. Res. Lett. 36, L15818.
Brown, S.S., Stutz, J., 2012. Nighttime radical observations and chemistry. Chem. Soc. Rev. 41, 6405–6447.
Chameides, W.L., 1986. Possible role of NO_3 in the nighttime chemistry of a cloud. J. Geophys. Res. 91, 5331–5337.
Chen, H., Varner, M.E., Gerber, R.B., Finlayson-Pitts, B.J., 2016. Reactions of methanesulfonic acid with amines and ammonia as a source of new particles in air. J. Phys. Chem. B 120, 1526–1536.
Chen, H., Chee, S., Lawler, M.J., Barsanti, K.C., Wong, B.M., Smith, J.N., 2018a. Size resolved chemical composition of nanoparticles from reactions of sulfuric acid with ammonia and dimethylamine. Aerosol Sci. Technol. 52, 1120–1133.
Chen, Y., Wolke, R., Ran, L., Birmili, W., Spindler, G., Schröder, W., et al., 2018b. A parameterization of the heterogeneous hydrolysis of N_2O_5 for mass-based aerosol models: improvement of particulate nitrate prediction. Atmos. Chem. Phys. 18, 673–689.
Cheng, Y., Zheng, G., Wei, C., Mu, Q., Zheng, B., Wang, Z., et al., 2016. Reactive nitrogen chemistry in aerosol water as a source of sulfate during haze events in China. Sci. Adv. 2, e1601530.
DePalma, J.W., Doren, D.J., Johnston, M.V., 2014. Formation and growth of molecular clusters containing sulfuric acid, water, ammonia, and dimethylamine. J. Phys. Chem. A 118, 5464–5473.
Ding, Z., Du, W., Wu, C., Cheng, C., Meng, J., Li, D., et al., 2020. Summertime atmospheric dicarboxylic acids and related SOA in the background region of Yangtze River Delta, China: implications for heterogeneous reaction of oxalic acid with sea salts. Sci. Total Environ. 143741.
Faxon, C.B., Allen, D.T., 2013. Chlorine chemistry in urban atmospheres: a review. Environ. Chem. 10, 221–233.
Feingold, G., 2002. Role of NO_3 in sulfate production in the wintertime northern latitudes. J. Geophys. Res. 107, 4640.
Gao, M., Carmichael, G.R., Wang, Y., Ji, D., Liu, Z., Wang, Z., 2016a. Improving simulations of sulfate aerosols during winter haze over Northern China: the impacts of heterogeneous oxidation by NO_2. Front. Environ. Sci. Eng. 10, 16.
Gao, M., Carmichael, G.R., Wang, Y., Saide, P.E., Yu, M., Xin, J., et al., 2016b. Modeling study of the 2010 regional haze event in the North China Plain. Atmos. Chem. Phys. 16, 1673–1691.
Gaston, C.J., Thornton, J.A., 2016. Reacto-diffusive length of N_2O_5 in aqueous sulfate- and chloride-containing aerosol particles. J. Phys. Chem. A 120, 1039–1045.
Ge, B., Xu, X., Ma, Z., Pan, X., Wang, Z., Lin, W., et al., 2019a. Role of ammonia on the feedback between AWC and inorganic aerosol formation during heavy pollution in the North China Plain. Earth Space Sci. 6, 1675–1693.
Ge, S., Wang, G., Zhang, S., Li, D., Xie, Y., Wu, C., et al., 2019b. Abundant NH_3 in China enhances atmospheric HONO production by promoting the heterogeneous reaction of SO_2 with NO_2. Environ. Sci. Technol. 53, 14339–14347.
Hu, D., Qiao, L., Chen, J., Ye, X., Yang, X., Cheng, T., et al., 2010. Hygroscopicity of inorganic aerosols: size and relative humidity effects on the growth factor. Aerosol Air Qual. Res. 10, 255–264.
Hung, H.M., Hoffmann, M.R., 2015. Oxidation of gas-phase SO_2 on the surfaces of acidic microdroplets: implications for sulfate and sulfate radical anion formation in the atmospheric liquid phase. Environmental Science & Technology. 49, 13768–13776.
Keene, W.C., Pszenny, A.A.P., Jacob, D.J., Duce, R.A., Galloway, J.N., Schultz-Tokos, J.J., et al., 1990. The geochemical cycling of reactive chlorine through the marine troposphere. Glob. Biogeochem. Cycles 4, 407–430.
Laskin, A., Gaspar, D.J., Wang, W., Hunt, S.W., Cowin, J.P., Colson, S.D., et al., 2003. Reactions at interfaces as a source of sulfate formation in sea-salt particles. Science. 301, 340–344.
Lehtipalo, K., Rondo, L., Kontkanen, J., Schobesberger, S., Jokinen, T., Sarnela, N., et al., 2016. The effect of acid-base clustering and ions on the growth of atmospheric nano-particles. Nat. Commun. 7, 11594.
Li, L., Chen, Z.M., Zhang, Y.H., Zhu, T., Li, S., Li, H.J., et al., 2007. Heterogeneous oxidation of sulfur dioxide by ozone on the surface of sodium chloride and its mixtures with other components. J. Geophys. Res. 112, D18301.
Li, K., Jacob, D.J., Liao, H., Shen, L., Zhang, Q., Bates, K.H., 2019. Anthropogenic drivers of 2013–2017 trends in summer surface ozone in China. Proc. Natl. Acad. Sci. U. S. A. 116, 422–427.
Liebmann, J., Sobanski, N., Schuladen, J., Karu, E., Hellén, H., Hakola, H., et al., 2019. Alkyl nitrates in the boreal forest: formation via the NO_3-, OH- and O_3-induced oxidation of biogenic volatile organic compounds and ambient lifetimes. Atmos. Chem. Phys. 19, 10391–10403.
Lin, Y.-C., Zhang, Y.-L., Fan, M.-Y., Bao, M., 2020. Heterogeneous formation of particulate nitrate under ammonium-rich regimes during the high-PM2.5 events in Nanjing, China. Atmos. Chem. Phys. 20, 3999–4011.
Ma, Q., He, H., Liu, Y., Liu, C., Grassian, V.H., 2013. Heterogeneous and multiphase formation pathways of gypsum in the atmosphere. Phys. Chem. Chem. Phys. 15, 19196–19204.
Ma, Q., Wu, Y., Fu, S., Zhang, D., Han, Z., Zhang, R., 2020. Pollution severity-dependent aerosol light scattering enhanced by inorganic species formation in Beijing haze. Sci. Total Environ. 719, 137545.
McDuffie, E.E., Fibiger, D.L., Dubé, W.P., Lopez-Hilfiker, F., Lee, B.H., Thornton, J.A., et al., 2018. Heterogeneous N_2O_5 uptake during winter: aircraft measurements during the 2015 WINTER campaign and critical evaluation of current parameterizations. J. Geophys. Res. Atmos. 123, 4345–4372.
Park, K., Kim, J.-S., Miller, A.L., 2008. A study on effects of size and structure on hygroscopicity of nanoparticles using a tandem differential mobility analyzer and TEM. J. Nanopart. Res. 11, 175–183.
Park, J., Jang, M., Yu, Z., 2017. Heterogeneous photo-oxidation of SO_2 in the presence of two different mineral dust particles: Gobi and Arizona dust. Environ. Sci. Technol. 51, 9605–9613.
Peng, C., Jing, B., Guo, Y.C., Zhang, Y.H., Ge, M.F., 2016. Hygroscopic behavior of multicomponent aerosols involving NaCl and dicarboxylic acids. J. Phys. Chem. A 120, 1029–1038.
Qiu, C., Zhang, R., 2013. Multiphase chemistry of atmospheric amines. Phys. Chem. Chem. Phys. 15, 5738–5752.
Qiu, C., Wang, L., Lal, V., Khalizov, A.F., Zhang, R., 2011. Heterogeneous reactions of alkylamines with ammonium sulfate and ammonium bisulfate. Environ. Sci. Technol. 45, 4748–4755.
Reilly, J.E., Rattigan, O.V., Moore, K.F., Judd, C., Eli Sherman, D., Dutkiewicz, V.A., et al., 2001. Drop size-dependent S(IV) oxidation in chemically heterogeneous radiation fogs. Atmos. Environ. 35, 5717–5728.
Rudich, Y., Talukdar, R.K., Ravishankara, A.R., 1998. Multiphase chemistry of NO_3 in the remote troposphere. J. Geophys. Res. Atmos. 103, 16133–16143.
Schütze, M., Herrmann, H., 2005. Uptake of the NO_3 radical on aqueous surfaces. J. Atmos. Chem. 52, 1–18.
Sun, W., Wang, D., Yao, L., Fu, H., Fu, Q., Wang, H., et al., 2019. Chemistry-triggered events of PM2.5 explosive growth during late autumn and winter in Shanghai, China. Environ Pollut. 254, 112864.
Tao, W., Su, H., Zheng, G.J., Wang, J.D., Wei, C., Liu, L.X., et al., 2020. Aerosol pH and chemical regimes of sulfate formation in aerosol water during winter haze in the North China Plain. Atmos. Chem. Phys. 20, 11729–11746.
Unger, N., Shindell, D.T., Koch, D.M., Streets, D.G., 2006. Cross influences of ozone and sulfate precursor emissions changes on air quality and climate. Proc. Natl. Acad. Sci. U. S. A. 103, 4377–4380.
Venkataraman, C., Mehra, A., Mhaskar, P., 2001. Mechanisms of sulphate aerosol production in clouds: effect of cloud characteristics and season in the Indian region. Tellus B. 53, 260–272.
Vu, T.V., Shi, Z., Cheng, J., Zhang, Q., He, K., Wang, S., et al., 2019. Assessing the impact of clean air action on air quality trends in Beijing using a machine learning technique. Atmos. Chem. Phys. 19, 11303–11314.
Wang, G.H., Zhou, B.H., Cheng, C.L., Cao, J.J., Li, J.J., Meng, J.J., et al., 2013. Impact of Gobi desert dust on aerosol chemistry of Xi'an, inland China during spring 2009: differences in composition and size distribution between the urban ground surface and the mountain atmosphere. Atmos. Chem. Phys. 13, 819–835.
Wang, G.H., Cheng, C.L., Huang, Y., Tao, J., Ren, Y.Q., Wu, F., et al., 2014. Evolution of aerosol chemistry in Xi'an, inland China, during the dust storm period of 2013-part 1: sources, chemical forms and formation mechanisms of nitrate and sulfate. Atmos. Chem. Phys. 14, 11571–11585.
Wang, G., Zhang, R., Gomez, M.E., Yang, L., Levy Zamora, M., Hu, M., et al., 2016. Persistent sulfate formation from London Fog to Chinese haze. Proc. Natl. Acad. Sci. U. S. A. 113, 13630–13635.
Wang, G., Zhang, F., Peng, J., Duan, L., Ji, Y., Marrero-Ortiz, W., et al., 2018a. Particle acidity and sulfate production during severe haze events in China cannot be reliably inferred by assuming a mixture of inorganic salts. Atmos. Chem. Phys. 18, 10123–10132.
Wang, J.F., Li, J.Y., Ye, J.H., Zhao, J., Wu, Y.Z., Hu, J.L., et al., 2020. Fast sulfate formation from oxidation of SO_2 by NO_2 and HONO observed in Beijing haze. Nat. Commun. 11: 2844.
Wang, H., Lu, K., Guo, S., Wu, Z., Shang, D., Tan, Z., et al., 2018b. Efficient N_2O_5 uptake and NO_3 oxidation in the outflow of urban Beijing. Atmos. Chem. Phys. 18, 9705–9721.
Warneck, P., 1999. The relative importance of various pathways for the oxidation of sulfur dioxide and nitrogen dioxide in sunlit continental fair weather clouds. Phys. Chem. Chem. Phys. 1, 5471–5483.
Wu, L., Sun, J., Zhang, X., Zhang, Y., Wang, Y., Zhong, J., et al., 2019. Aqueous-phase reactions occurred in the PM2.5 cumulative explosive growth during the heavy pollution episode (HPE) in 2016 Beijing wintertime. Tellus B Chem. Phys. Meteorol. 71, 1–15.
Wu, C., Wang, G.H., Li, J., Li, J.J., Cao, C., Ge, S.S., et al., 2020a. Non-agricultural sources dominate the atmospheric NH3 in Xi'an, a megacity in the semi-arid region of China. Sci. Total Environ. 722, 137756.
Wu, C., Zhang, S., Wang, G., Lv, S., Li, D., Liu, L., et al., 2020b. Efficient heterogeneous formation of ammonium nitrate on the saline mineral particle surface in the atmosphere of East Asia during dust storm periods. Environ Sci Technol. 54, 15622–15630.
Xie, Y.N., Wang, G.H., Wang, X.P., Chen, J.M., Chen, Y.B., Tang, G.Q., et al., 2020. Nitrate-dominated PM2.5 and elevation of particle pH observed in urban Beijing during the winter of 2017. Atmos. Chem. Phys. 20, 5019–5033.
Xue, J., Yu, X., Yuan, Z.B., Griffith, S.M., Lau, A.K.H., Seinfeld, J.H., et al., 2019. Efficient control of atmospheric sulfate production based on three formation regimes. Nat. Geosci. 12, 977–982.
Yang, W., Ma, Q., Liu, Y., Ma, J., Chu, B., Wang, L., et al., 2018. Role of NH_3 in the heterogeneous formation of secondary inorganic aerosols on mineral oxides. J. Phys. Chem. A 122, 6311–6320.
Zhai, S., Jacob, D.J., Wang, X., Shen, L., Li, K., Zhang, Y., et al., 2019. Fine particulate matter (PM2.5) trends in China, 2013–2018: separating contributions from anthropogenic emissions and meteorology. Atmos. Chem. Phys. 19, 11031–11041.
Zhang, R., Jing, J., Tao, J., Hsu, S.C., Wang, G., Cao, J., et al., 2013. Chemical characterization and source apportionment of PM2.5 in Beijing: seasonal perspective. Atmos. Chem. Phys. 13, 7053–7074.
Zhang, Q., Zheng, Y.X., Tong, D., Shao, M., Wang, S.X., Zhang, Y.H., et al., 2019. Drivers of improved PM2.5 air quality in China from 2013 to 2017. Proc. Natl. Acad. Sci. U. S. A. 116, 24463–24469.
Zheng, B., Tong, D., Li, M., Liu, F., Hong, C., Geng, G., et al., 2018. Trends in China's anthropogenic emissions since 2010 as the consequence of clean air actions. Atmos. Chem. Phys. 18, 14095–14111.